

# Hyperfine interactions in $\text{Ho}(\text{Fe}_{1-x}\text{Co}_x)_2$ compounds at 295 K

Mikołaj Bednarski,  
Paweł Stoch,  
Wiktor Bodnar,  
Piotr Zachariasz,  
Jarosław Pszczola,  
Jan Suwalski

**Abstract.** Synthesis of  $\text{Ho}(\text{Fe}_{1-x}\text{Co}_x)_2$  intermetallic compounds, studies of their crystal structure and  $^{57}\text{Fe}$  Mössbauer effect analysis were carried out at 295 K. X-ray measurements evidence a pure cubic  $Fd\bar{3}m$ , C15,  $\text{MgCu}_2$ -type Laves phase. The unit cell parameter decreases non-linearly with composition parameter  $x$ . Mössbauer effect spectra for the  $\text{Ho}(\text{Fe}_{1-x}\text{Co}_x)_2$  series were composed of a number of locally originated subspectra due to random Fe/Co nearest neighbourhoods. Hyperfine interaction parameters, i.e. isomer shift, the magnetic hyperfine field and a quadrupole interaction parameter were determined from the fitting procedure of the spectra, for both the individual nearest neighbourhoods, and for the sample as bulk. As a consequence of Fe/Co substitution a Slater-Pauling type curve for the average magnetic hyperfine field vs.  $x$  is observed. The correlation between the local magnetic hyperfine fields and the average magnetic hyperfine fields is related to weak and strong ferromagnetism of the transition metal sublattice.

**Key words:** intermetallics • crystal structure • Laves phase • Mössbauer effect • hyperfine interaction • Slater-Pauling dependence

M. Bednarski, W. Bodnar, J. Pszczola<sup>✉</sup>  
Faculty of Physics and Applied Computer Science,  
AGH University of Science and Technology,  
30 A. Mickiewicza Ave., 30-059 Kraków, Poland,  
Tel.: +48 12 617 2990, Fax: +48 12 634 0010,  
E-mail: pszczola@agh.edu.pl

P. Stoch  
Institute of Atomic Energy,  
05-400 Otwock-Świerk, Poland  
and Faculty of Material Science and Ceramics,  
AGH University of Science and Technology,  
30 A. Mickiewicza Ave., 30-059 Kraków, Poland

P. Zachariasz, J. Suwalski  
Institute of Atomic Energy,  
05-400 Otwock-Świerk, Poland

Received: 15 April 2010  
Accepted: 8 June 2010

## Introduction

Heavy rare earth (R) – transition metal (M) intermetallic compounds with stoichiometric formula  $\text{RM}_2$  have been widely studied for scientific and practical reasons [2–4, 23]. The ferrimagnetic properties of these materials depend on the rare earth constituent ( $4f5d$  electrons) as well as on the transition metal constituent ( $3d$  electrons) [5]. Previously, the significance of the  $3d$  electrons has been experimentally studied in the  $\text{Dy}(\text{Fe}_{1-x}\text{Co}_x)_2$  intermetallic series using the  $^{57}\text{Fe}$  Mössbauer effect [9, 10, 19]. It has been found that the magnetic hyperfine field  $\mu_0 H_{\text{hf}}$  ( $\mu_0$  is the magnetic permeability) observed at  $^{57}\text{Fe}$  nuclei treated as a function of the average number  $n$  of  $3d$  electrons in the transition metal  $3d$  band follows a Slater-Pauling type dependence [9, 10, 19]. With this in mind it was also interesting to test less known hyperfine interactions in  $\text{Ho}(\text{Fe}_{1-x}\text{Co}_x)_2$  compounds. Recently, R-M intermetallics are used as magnetostrictive constituents of novel magnetoelectric composites and laminates [8]. So, it is interesting to study  $\text{Ho}(\text{Fe}_{1-x}\text{Co}_x)_2$  compounds, which can be treated as potential constituents of magnetoelectric materials.

## Materials and X-ray studies

Polycrystalline materials  $\text{Ho}(\text{Fe}_{1-x}\text{Co}_x)_2$  ( $x = 0, 0.2, 0.3, 0.5, 0.7, 0.8, 0.9$  and  $1.0$ ) were synthesized by arc melting

with contact-less ignition in a high purity argon atmosphere, applying appropriate amounts of Ho (99.95% purity), Fe and Co (all 99.99% purity) metals [18]. The obtained ingots were annealed in vacuum at 1200 K for 1 h and then cooled down along with the furnace (approximate cooling rate: 250 K/h).

The crystal structure of the post-annealed compounds was studied with standard X-ray powder diffraction measurements using  $\text{MoK}_\alpha$  radiation. The X-ray diffractograms (Fig. 1) measured for these compounds were numerically analyzed using a Rietveld-type procedure adopting both the  $\text{K}_{\alpha_1}$  (wavelength  $\lambda_1 = 0.70930 \text{ \AA}$ ) and  $\text{K}_{\alpha_2}$  (wavelength  $\lambda_2 = 0.71359 \text{ \AA}$ ) X-ray lines [14, 15]. For all compounds of the tested series a clean cubic Laves phase with  $Fd\bar{3}m$ ,  $\text{MgCu}_2$ -type, C15 crystal structure was evidenced. The C15-type Laves phase has been described in detail elsewhere [11].

It can be noted that in this crystal structure each transition metal atom has six transition metal atoms as the nearest neighbours [11].

As the atomic radius of Fe ( $r_{\text{Fe}} = 1.72 \text{ \AA}$ ) is larger when compared to the radius of Co ( $r_{\text{Co}} = 1.67 \text{ \AA}$ ), the determined unit cell parameter, described by the fitted numerical formula:  $a(x) = (7.310 - 0.018x - 0.110x^2) \text{ \AA}$ , reduces softly non-linearly with parameter  $x$  (Fig. 2, curve 1) [21]. This formula, which was obtained by using a least squares fitting procedure, follows the experimental points satisfactorily. An appreciated maximal error  $\Delta a$  of experimental points (not presented in the figure) equals  $0.0013 \text{ \AA}$ . The determined values for the borderline compounds of the studied series coincide satisfactorily with the existing literature data (open marks in Fig. 2, curve 1) [12, 13, 20, 22, 23].

Figure 2 also presents the calculated unit cell volumes, described by the numerical formula  $V(x) = (390.611 - 2.449x - 17.789x^2) [\text{\AA}^3]$  (curve 2), and volumes per atom  $w(x) = (16.275 - 0.102x - 0.741x^2) [\text{\AA}^3]$  (curve 3). The observed convex deviation  $a(x)$ ,  $V(x)$  and  $w(x)$  from Vegard's rule, which is typical for R-M intermetallics, can presumably be ascribed to a magnetovolume effect.

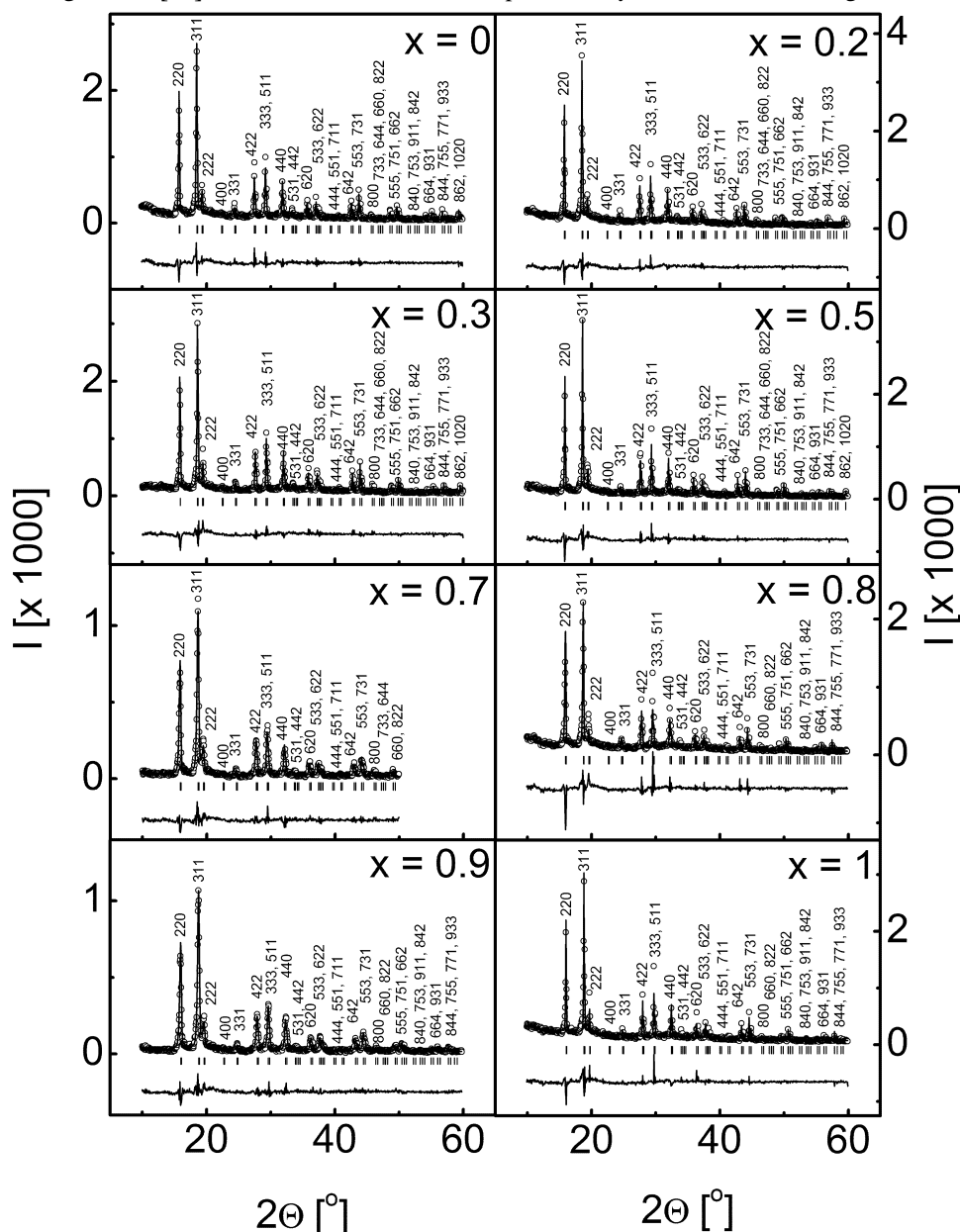
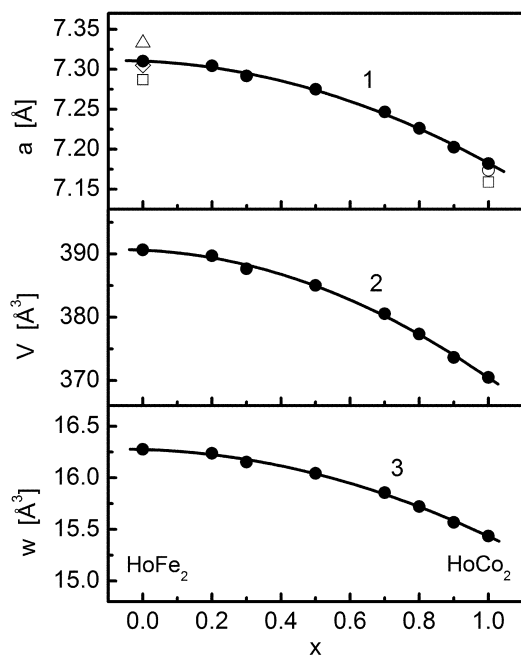


Fig. 1. X-ray patterns of the  $\text{Ho}(\text{Fe}_{1-x}\text{Co}_x)_2$  intermetallic series at 295 K.



**Fig. 2.** The unit cell parameters (curve 1), the unit cell volumes (curve 2) and the volumes per atom (curve 3) of the  $\text{Ho}(\text{Fe}_{1-x}\text{Co}_x)_2$  intermetallics (295 K). Open marks taken from the literature [12, 13, 20, 22, 23].

## Mössbauer effect

### Spectra and fitting

The  $^{57}\text{Fe}$  Mössbauer effect spectra (Fig. 3), were measured at 295 K by using a standard transmission technique with a  $^{57}\text{Co}$  in Pd source. The spectra were fitted

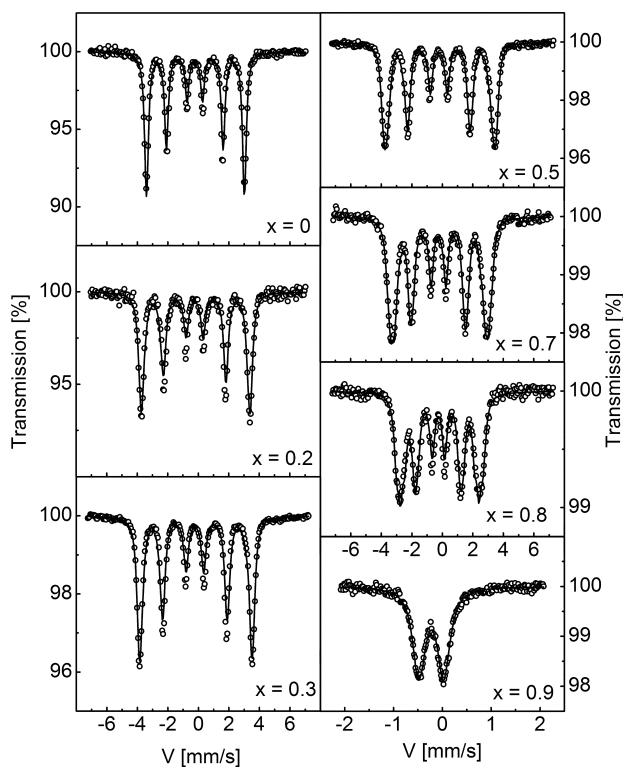


**Fig. 3.**  $^{57}\text{Fe}$  Mössbauer effect spectra of the  $\text{Ho}(\text{Fe}_{1-x}\text{Co}_x)_2$  intermetallics (295 K).

considering both the  $[100]$  easy axis of magnetization and the assumed random distribution of Fe and Co atoms in the transition metal sublattice.

The random distribution of atoms in the sublattice causes different neighbourhoods of the probed  $^{57}\text{Fe}$  atoms. Specifically, iron atom can be surrounded by  $(6-k)$  iron atoms and  $k$  cobalt atoms ( $k = 0, 1, 2, \dots, 6$ ) as the nearest neighbours. Particular Fe/Co neighbourhoods locally determine their own Mössbauer effect subspectra which contribute to the resulting measured Mössbauer effect pattern and thus introduce, which correspond to these subspectra, local-type hyperfine interaction parameters. The probability of particular nearest neighbourhoods and thus subspectra  $P(6;k) = \{[6! / (6-k)!k!] \cdot [(1-x)^{6-k}x^k]\}$  is described by the Bernoulli formula, here in the form adapted for the  $\text{Ho}(\text{Fe}_{1-x}\text{Co}_x)_2$  series [7]. A fitting procedure was performed, assuming that the amplitudes  $A(k)$  of the particular subspectra follow the probabilities  $P(6;k)$ .

In order to reduce the number of fitted parameters, neighbourhoods with probabilities of less than 0.1 of maximal probability were not considered. Consequently, the remaining probabilities were normalized again.

### Local hyperfine magnetic fields

The magnetic hyperfine fields  $\mu_0 H_{\text{hf}}$  corresponding to the individual subspectra of the  $\text{Ho}(\text{Fe}_{1-x}\text{Co}_x)_2$  series obtained from the fitting procedure ascribed to particular numbers  $k$  are presented in Fig. 4. These  $\mu_0 H_{\text{hf}}(k)$  dependencies, determined for particular compounds of the series, are marked with the  $x$ -parameter. Moreover, Fig. 4 (dashed line), shows the magnetic hyperfine field  $\mu_0 H_{\text{hf}}$ , arithmetically averaged over  $x$ . The averaged

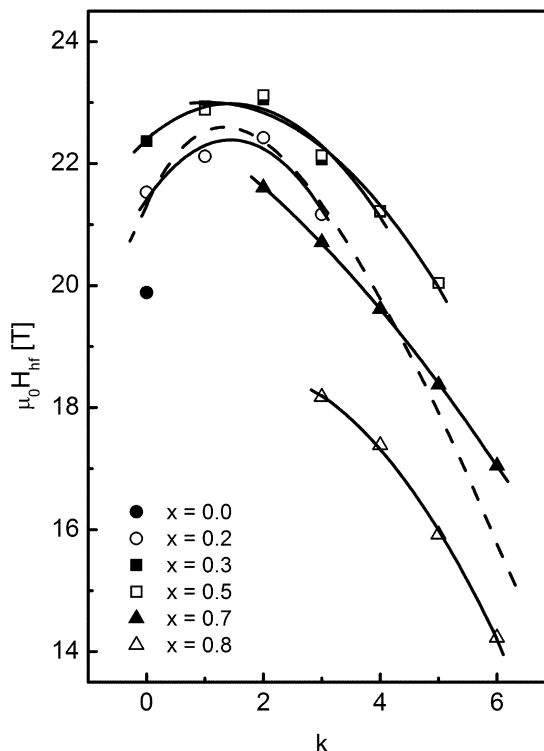


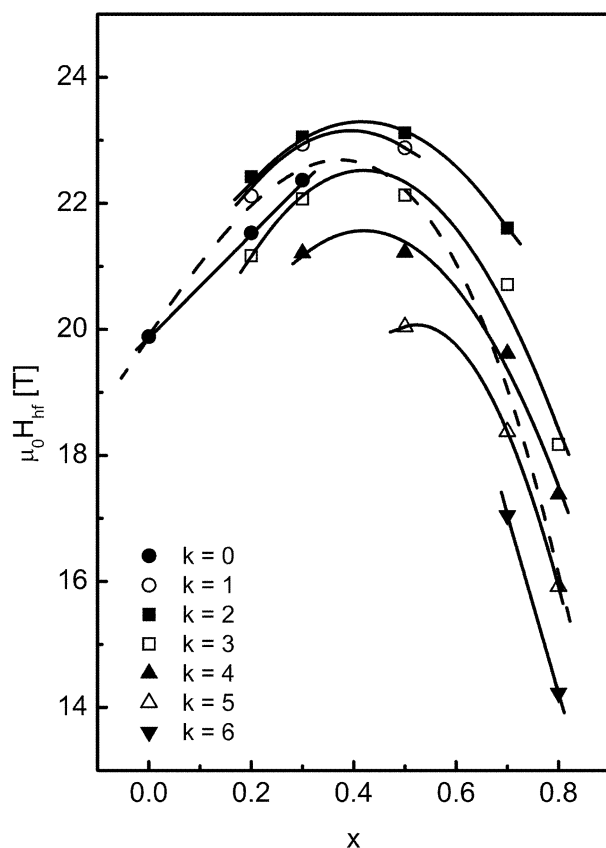
**Fig. 4.** Magnetic hyperfine fields for the  $\text{Ho}(\text{Fe}_{1-x}\text{Co}_x)_2$  series: local fields  $\mu_0 H_{\text{hf}}$  labelled by  $x$  as function of  $k$ , the average values presented by dashed line.

magnetic hyperfine field  $\mu_0 H_{\text{hf}}$  was fitted using the numerical formula:  $\mu_0 H_{\text{hf}}(k) = (21.326 + 2.089k - 1.004k^2 + 0.122k^3 - 0.006k^4) T$ .

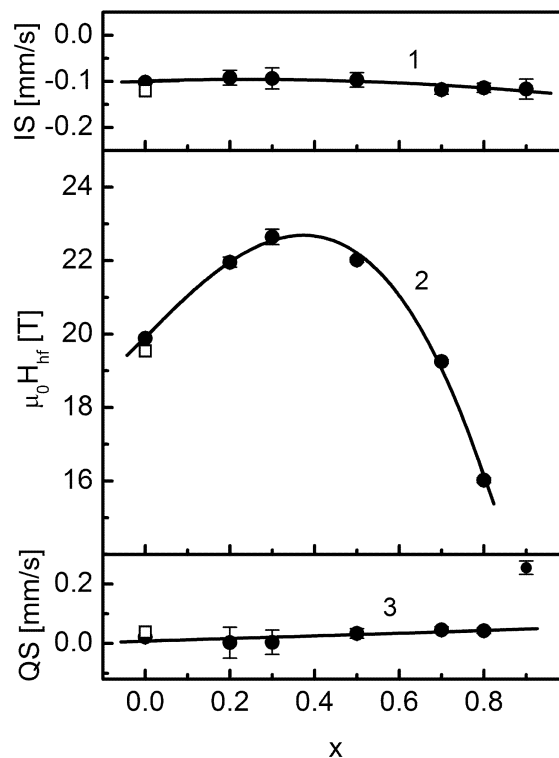
It can be noted that the individual dependencies in Fig. 4 contribute to the arithmetical average dependence, which, being locally originated, resembles a Slater-Pauling dependence.

Figure also contains a value  $\mu_0 H_{\text{hf}}(k = 0)$  obtained for  $\text{HoFe}_2$ , the starting compound of the series. It can be seen that the values  $\mu_0 H_{\text{hf}}(k = 0)$  determined for the  $\text{Ho}(\text{Fe}_{0.8}\text{Co}_{0.2})_2$  and  $\text{Ho}(\text{Fe}_{0.7}\text{Co}_{0.3})_2$  compounds are situated above the point for  $\text{HoFe}_2$ . Additionally, the  $\mu_0 H_{\text{hf}}(k = 0)$  value, corresponding to  $\text{Ho}(\text{Fe}_{0.7}\text{Co}_{0.3})_2$ , is higher compared to the value obtained for  $\text{Ho}(\text{Fe}_{0.8}\text{Co}_{0.2})_2$ . This tendency to grow is presumably caused by a growing content of Co-atoms with  $x$  in the next nearest neighbour coordination. Since the number of parameters during the fitting procedure had to be limited, the next nearest coordination was not considered.

In Fig. 5 locally originated, magnetic hyperfine field data are presented again. These  $\mu_0 H_{\text{hf}}$  dependencies ascribed to the corresponding  $k$  values, are shown as functions of the composition parameter  $x$ . The dashed line, which follows the numerical formula  $\mu_0 H_{\text{hf}}(x) = (19.899 + 12.106x - 4.858x^2 - 20.229x^3) T$ , corresponds to average magnetic hyperfine fields calculated for each  $x$  using the Bernoulli distribution formula [7]. Also in this case the average  $\mu_0 H_{\text{hf}}$  dependence is similar to a Slater-Pauling type curve. The maximum value of the  $\mu_0 H_{\text{hf}}$  field is situated at  $0.3 < x < 0.4$ .



**Fig. 5.** Magnetic hyperfine fields for the  $\text{Ho}(\text{Fe}_{1-x}\text{Co}_x)_2$  series: local fields  $\mu_0 H_{\text{hf}}$  labelled by  $k$  as function of  $x$ , the average values presented by dashed line.



**Fig. 6.** Hyperfine interaction parameters of the  $\text{Ho}(\text{Fe}_{1-x}\text{Co}_x)_2$  series. Open symbols denote literature data [22].

#### Average parameters

The average hyperfine interaction parameters, i.e. the isomer shift IS (with respect to armco iron foil, at 300 K), the magnetic hyperfine field  $\mu_0 H_{\text{hf}}$  and the quadrupole interaction parameter QS [28], weighted by subspectra amplitude, which were calculated for the  $\text{Ho}(\text{Fe}_{1-x}\text{Co}_x)_2$  series at 295 K, are presented in Fig. 6.

The isomer shift IS is described by the numerical formula  $\text{IS}(x) = (-0.099 + 0.028x - 0.059x^2) \text{ mm/s}$  (Fig. 6, line 1).

The obtained isomer shift correlates linearly with the volume per atom, following the numerical formula  $\text{IS}(x) = [-0.744 + 0.040w(x)] \text{ mm/s}$ , as presented in Fig. 7.

It has been previously deduced that, in the case of an  $^{57}\text{Fe}$  nucleus, an increase in the  $d$ -electron density in an iron atom causes a growth in isomer shift, whereas an increase in  $s$ -electron density triggers a reduction in

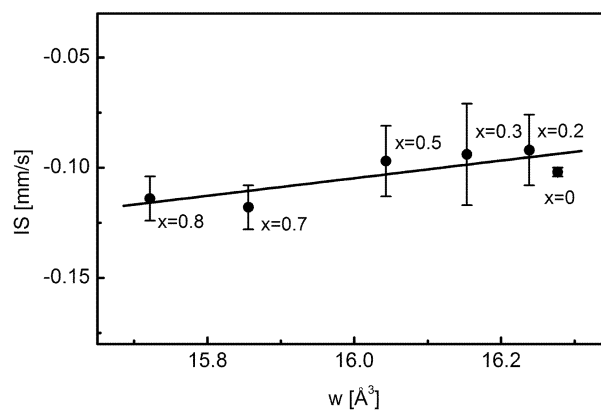


**Fig. 7.** The correlation between isomer shift  $\text{IS}(x)$  and  $w(x)$  the unit cell volume per atom. Points labelled by  $x$  values.

isomer shift [17, 27]. In the studied series the isomer shift decreases with growing  $x$  and also reduces with a decreasing  $w$ -volume (Fig. 7). It can be expected that the reduction in the  $w$ -volume with  $x$  causes an increase in both  $d$ -electron and  $s$ -electron density in the Fe atom. As well, in the  $\text{Ho}(\text{Fe}_{1-x}\text{Co}_x)_2$  series the number of  $s$ -electrons per atom is constant and the number of  $d$ -electrons per atom considerably increases with  $x$ , and the isomer shift decreases. This does not contradict the findings of other papers [17, 27]. Presumably, as a result of Fe/Co replacement, i.e. of the M-M atom distance reduction and of the growing number of  $3d$  electrons, these electrons gradually approach more of a band character and the probability of them residing in an Fe atom decreases with  $x$ , reducing the isomer shift.

The average  $\mu_0 H_{\text{hf}}(x)$  dependence (Fig. 6, line 2) is described by the same numerical formula as used in Fig. 5. Figure 6 also contains fragmentary literature data at  $x = 0$ , which fit well to the results obtained [22].

The average magnetic hyperfine field follows a Slater-Pauling type dependence. At first, behaviour of a weak ferromagnetic type of the transition metal sublattice is observed. That is, two (weighted for Fe and Co contribution)  $3d$  subbands with opposite spin are gradually filled up with  $x$  and the spin population of the majority  $3d$  subband predominates [1]. Consequently, the magnetic hyperfine field across the  $\text{Ho}(\text{Fe}_{1-x}\text{Co}_x)_2$  series increases with  $x$  and the maximum value of the field is approached for  $0.3 < x < 0.4$ . In this composition area the filling up of the majority  $3d$  subband by  $3d$  electrons is terminated.

Further, Co-substitution introduces behaviour of a strong ferromagnetic type of the M-sublattice [1]. The filling-up of the minority  $3d$  subband is further continued, and, as a result, the observed field decreases gradually with  $x$ . The Curie temperatures for the  $\text{Ho}(\text{Fe}_{1-x}\text{Co}_x)_2$  series are not yet known. Only Curie temperatures for the borderline compounds of the series were determined, namely  $T_C = 612$  K [12, 16, 23] for  $\text{HoFe}_2$  and  $T_C = 78$  K [6, 24–26, 29] for  $\text{HoCo}_2$ . Concerning the Mössbauer effect spectrum (the quadrupole doublet) for  $x = 0.9$ , it can be expected that the Curie temperature for the sample  $\text{Ho}(\text{Fe}_{0.1}\text{Co}_{0.9})_2$  is below the temperature of measurement. The quadrupole parameter QS increases slightly with  $x$  and follows the numerical formula:  $\text{QS}(x) = (0.008 + 0.044x)$  mm/s (Fig. 6, line 3).

### Correlation among magnetic fields

It is interesting to compare the average local magnetic hyperfine field  $\mu_0 H_{\text{hf}}$  as a function of number  $k$ , (Fig. 4, dashed line) and the average  $\mu_0 H_{\text{hf}}$  field as a function of composition parameter  $x$  (Fig. 5, dashed line). The points of the resulting correlation between  $\mu_0 H_{\text{hf}}(x)$  and  $\mu_0 H_{\text{hf}}(k)$  are marked by numbers  $x$  and  $k$ .

The above-mentioned  $\mu_0 H_{\text{hf}}(k)$  dependence correlated with  $\mu_0 H_{\text{hf}}(x)$  dependence is presented as two sections 1 and 2, described by the numerical formulae:  $\mu_0 H_{\text{hf}}(k) = [0.560 \mu_0 H_{\text{hf}}(x) + 10.742] T$  (Fig. 8, line 1) and  $\mu_0 H_{\text{hf}}(k) = [0.572 \mu_0 H_{\text{hf}}(x) + 8.584] T$  (Fig. 8, line 2), correspondingly.

It can be noted that section 1 corresponds to the weak ferromagnetism, and section 2 corresponds to

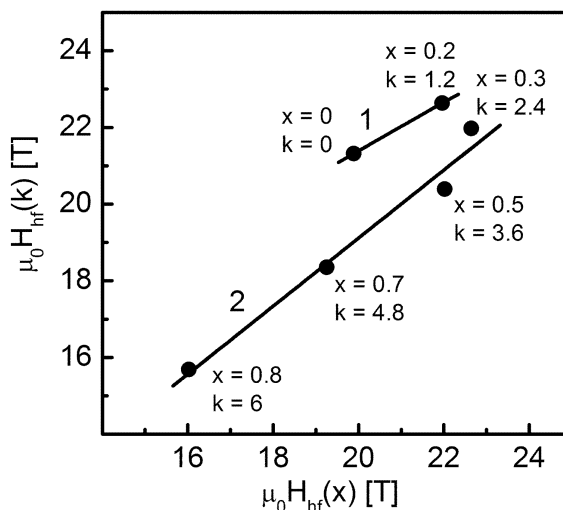


**Fig. 8.** Correlations between magnetic hyperfine fields  $\mu_0 H_{\text{hf}}(k)$  and  $\mu_0 H_{\text{hf}}(x)$ . Points labelled by  $x$  and  $k$  values.

the strong ferromagnetism observed in the transition metal sublattice.

### Summary

Fe/Co replacement in the  $\text{Ho}(\text{Fe}_{1-x}\text{Co}_x)_2$  series introduces an additional  $3d$  electron per transition metal atom. As a result, it reduces the lattice parameter, and the unit cell volume, thus reducing with  $x$  the average distance between the  $3d$  transition metal nearest neighbours. Consequently, the band structure, especially the  $3d$  band structure, along with all observed physical properties, including hyperfine interactions are modified across the series.

So, Fe/Co replacement introduces differences in the local surroundings of the probed iron atoms. The magnetic hyperfine fields  $\mu_0 H_{\text{hf}}$ , corresponding to different Fe/Co neighbourhoods presented against the number  $k$  labeled by the  $x$ -parameter, create fragments of local type Slater-Pauling dependencies (Fig. 4). The averaged  $\mu_0 H_{\text{hf}}$  dependence follows a Slater-Pauling type curve vs.  $k$ . Each Fe/Co neighbourhood of the probed Fe atom, characterized by the  $k$  number, produces its own local  $\mu_0 H_{\text{hf}}$  dependence as a function of  $x$ . These dependencies resemble fragments of a Slater-Pauling type curve (Fig. 5). The averaged dependence  $\mu_0 H_{\text{hf}}(x)$ , corresponding to the sample as bulk, has a shape typical of a Slater-Pauling curve.

It is worth noticing that the average value of  $\mu_0 H_{\text{hf}}(k)$  (taken from Fig. 4) and the average value of  $\mu_0 H_{\text{hf}}(x)$  (taken from Fig. 5) correlate linearly, as presented in Fig. 8, line 1 and 2. These correlations support additionally the idea that locally produced magnetic hyperfine fields distribute following a Slater-Pauling type dependence, as do the average fields characteristic of the sample as bulk.

Thus, it can be cautiously concluded that the local magnetic hyperfine field  $\mu_0 H_{\text{hf}}$  obeys weak ferromagnetism conditions (the increasing part of the curves), and strong ferromagnetism conditions (the decreasing part of the curves) in the transition metal sublattice. This result may be helpful both in further band type calculations and in potential applications of  $\text{Ho}(\text{Fe}_{1-x}\text{Co}_x)_2$

intermetallics as, for instance, constituents of the novel magnetoelectric media.

**Acknowledgment.** Supported partially by the Ministry of Science and Higher Education, project no. R015000504 and in part by AGH, projects no. 10.10.220.476 and no. 11.11.220.01.

## References

- Barbara B, Gignoux D, Vettier C (1988) Lectures on modern magnetism. Science Press Beijing, Berlin-Heidelberg
- Burzo E, Chełkowski A, Kirchmayr HR, Madelung O, Wijn HPJ (eds) (1990) Landolt-Bornstein numerical data and functional relationships in science and technology. New Series, Group III, Vol. 19, subvol. d2. Springer, Berlin
- Burzo E, Kirchmayr HR, Gnschneider KA Jr, Eyring L (eds) (1989) Handbook on the physics and chemistry of rare earths. Vol. 12, North-Holland Publishing Co, Amsterdam
- Buschow KHJ (1980) Rare earth compounds. In: Wohlfarth EP (ed) Ferromagnetic materials. Vol. 1, North-Holland Publishing Co, Amsterdam, pp 297–414
- Campbell IA (1972) Indirect exchange for rare earths in metals. *J Phys F: Met Phys* 2:L47–L50
- Cuong TD, Havela L, Sechovsky V, Arnold Z, Kamarad J, Duc NH (1998) Evolution of magnetism in  $\text{Ho}(\text{Co}_{1-x}\text{Si}_x)_2$  compounds. *J Magn Magn Mater* 177/181:597–598
- Feller W (1961) An introduction to probability theory and its applications, 2nd ed. Vol. 1. Wiley, London, pp 175–189
- Fiebig M (2005) Revival of the magnetoelectric effect. *J Phys D: Appl Phys* 38:R123–R152
- Gicala B, Pszczoła J, Kucharski Z, Suwalski J (1994) Two Slater-Pauling dependences for Dy-3d metal compounds. *Phys Lett A* 185:491–494
- Gicala B, Pszczoła J, Kucharski Z, Suwalski J (1995) Magnetic hyperfine fields of  $\text{Dy}_x(\text{Fe-Co})_y$  compounds. *Solid State Commun* 96:511–515
- Laves F (1939) Kristallographie der Legierungen. *Naturwissenschaften* 27:65–73
- Moreau JM, Michel C, Simmons M, O’Keefe TJ, James WJ (1971) Neutron diffraction study of the Ho-Fe system. *J Phys Colloques* 32:C1-670–C1-671
- Morozkin AV, Seropegin YuD, Gribanov AV, Barakatova JM (1997) Analysis of the melting temperatures of  $\text{RT}_2$  compounds ( $\text{MgCu}_2$  structure) ( $\text{R} = \text{rare earth}$ ,  $\text{T} = \text{Mn, Fe, Co, Ni, Ru, Rh, Pd, Os, Ir, Pt}$ ) and  $\text{RT}_2\text{X}_2$  compounds ( $\text{R} = \text{La, Ce, Sm, Er}$ ;  $\text{T} = \text{Mn, Fe, Co, Ni, Cu, Ru, Rh, Pd, Pt}$ ;  $\text{X} = \text{Si, Ge}$ ). *J Alloys Compd* 256:175–191
- Rietveld HM (1969) A profile refinement method for nuclear and magnetic structures. *J Appl Crystallogr* 2:65–71
- Rodriguez-Carvajal J (1993) Recent advances in magnetic structure determination by neutron powder diffraction. *Physica B* 192:55–69
- Sarkar D, Segnan R, Cornell EK *et al.* (1974) Crystal field in amorphous rare-earth-iron alloys. *Phys Rev Lett* 32:542–544
- Shimotomai M, Doyama M (1981) Quadrupole interaction of  $^{57}\text{Fe}$  in  $\alpha\text{-Sn}$ . *Hyperfine Interact* 9:329–332
- Stoch P, Onak M, Pańta A, Pszczoła J, Suwalski J (2002) Synthesis and crystal structure of  $\text{Dy}(\text{Fe-Co-Al})_2$ . IEA Monographs, Vol. 5. Instytut Energii Atomowej, Otwock-Świerk (in Polish)
- Stoch P, Pszczoła J, Guzdek P, Chmista J, Pańta A (2005) Electrical resistivity studies of  $\text{Dy}(\text{Fe}_{1-x}\text{Co}_x)_2$  compounds. *J Alloys Compd* 394:116–121
- Streltsov VA, Ishizawa N (1999) Synchrotron X-ray analysis of the electron density in  $\text{HoFe}_2$ . *Acta Crystallogr B* 55:321–326
- Table of periodic properties of the elements (1980) Sargent-Welch Scientific Company, Skokie
- Tang YJ, Luo HL, Gao LF, Pan SM (1995) Mössbauer studies of  $\text{R}(\text{Fe}_{1-x}\text{Mn}_x)_2$  ( $\text{R} = \text{Tb, Ho}$ ) intermetallic compounds. *J Mater Sci Lett* 14:705–707
- Taylor KNR (1971) Intermetallic rare-earth compounds. *Adv Phys* 20:551–660
- Tohei T, Wada H (2004) Change in the character of magnetocaloric effect with Ni substitution in  $\text{Ho}(\text{Co}_{1-x}\text{Ni}_x)_2$ . *J Magn Magn Mater* 280:101–107
- Uchima K, Nakama T, Takaesu Y *et al.* (2006) Transport properties of  $\text{Y}_{1-x}\text{R}_x\text{Co}_2$  ( $\text{R} = \text{Er, Ho}$ ) in magnetic field. *J Alloys Compd* 408/412:368–370
- Van der Kraan AM, Gubbens PCM (1974) Mössbauer study of the ternary system  $\text{Ho}(\text{Fe, Co})_2$ . *J Phys Colloques* 35:C6-469–C6-472
- Van der Woude F, Sawatzky GA (1974) Mössbauer effect in iron and dilute iron based alloys. *Phys Rep* 12:335–374
- Wertheim GK (1964) Mössbauer effect: principles and applications. Academic Press, New York, pp 59–71
- Yagasaki K, Misashi M, Notsu S *et al.* (2004) Transport properties of  $\text{Y}_{1-x}\text{Ho}_x\text{Co}_2$  in magnetic field. *J Magn Magn Mater* 272/276:E345–E346